

# Polymers with attractive interactions on the Husimi lattice

Pablo Serra\*

*Facultad de Matemática, Astronomía y Física  
Universidad Nacional de Córdoba  
Ciudad Universitaria - 5000 Córdoba  
Argentina*

Jürgen F. Stilck†

*Instituto de Física  
Universidade Federal Fluminense  
Av. Litorânea s/n  
24210-340 - Niterói, RJ  
Brazil*

Welchy L. Cavalcanti and Kleber D. Machado‡

*Departamento de Física  
Universidade Federal de Santa Catarina  
88.040-900 - Florianópolis - SC  
Brazil*

(Dated: June 23, 2018)

We obtain the solution of models of self-avoiding walks with attractive interactions on Husimi lattices built with squares. Two attractive interactions are considered: between monomers on first-neighbor sites and not consecutive along a walk and between bonds located on opposite edges of elementary squares. For coordination numbers  $q > 4$ , two phases, one polymerized the other non-polymerized, are present in the phase diagram. For small values of the attractive interaction the transition between those phases is continuous, but for higher values a first-order transition is found. Both regimes are separated by a tricritical point. For  $q=4$  a richer phase diagram is found, with an additional (dense) polymerized phase, which is stable for sufficiently strong interactions between bonds. The phase diagram of the model in the three-dimensional parameter space displays surfaces of continuous and discontinuous phase transitions and lines of tricritical points, critical endpoints and triple points.

PACS numbers: 05.50.+q, 61.41.+e, 64.60.Ht

## I. INTRODUCTION AND DEFINITION OF THE MODEL

Self-avoiding walks have been found to be useful models for the study of the behavior of polymers for quite a long time [1]. The self-avoidance constraint in general makes these models difficult to solve on regular lattices. On lattices with hierarchical treelike structure, however, like the Bethe [2] and the Husimi [3] lattices, it is not difficult to solve such models exactly. From the point of view of critical phenomena, these solutions lead to classical or ideal chain critical exponents, but non-universal features of the phase diagram may be closer to the ones observed on regular lattices than those provided by the usual mean-field methods [4].

The effect of monomer-solvent interactions on the behavior of polymers diluted in poor solvents may be in-

cluded in the model by allowing attractive interactions between segments of the chains. This induces a competition between repulsive, excluded volume interactions and the attractive short range interactions. As these latter interactions become sufficiently strong, the chains may change from an extended to a collapsed state [5]. While this collapse transition, usually identified with the  $\Theta$ -point, appears as a tricritical point in mean-field approximations and non-classical approximations on three-dimensional lattices, in two dimensions the situation does not seem to be so simple. Transfer-matrix calculations [6] and exact Bethe-ansatz results [7] for a  $O(n)$  model with four-spin interactions on the square lattice lead two phase diagrams where the second order transition line between the polymerized and non-polymerized phases ends at a multicritical point whose precise nature is not clear from these calculations, but which is definitely not a tricritical point. In the limit  $n \rightarrow 0$  this model corresponds to self-avoiding walks with attractive interactions between bonds of the walk which are located on opposite edges of elementary squares of the lattice. The four-spin interactions in the magnetic model are related to interactions between bonds on the corresponding polymer model. On the other hand, studies of the behavior of self-avoiding

---

\*Electronic address: serra@famaf.unc.edu.ar;  
URL: <http://tero.fis.uncor.edu/~serra>

†Electronic address: jstilck@if.uff.br

‡Electronic address: kleber@fisica.ufsc.br

walks on the square lattice with attractive interactions between monomers located on first-neighbor sites but not consecutive along the walk point to a tricritical collapse transition [8]. The main motivation of this work was to address the question of apparently quite similar models of attractive walks (bonds or monomers interacting) leading to qualitatively distinct phase diagrams. The problem of models with interactions between monomers or bonds only on Husimi lattices was considered in the literature [9, 10, 11]. On a four coordinated ( $q = 4$ ) Husimi tree, the phase diagram of the model with monomer-monomer interactions is qualitatively similar to the one found in general when  $q > 4$ . In the parameter space defined by the activity of a monomer ( $x$ ) and the Boltzmann factor of the elementary interaction between bonds ( $\omega$ ), a non-polymerized phase is stable at low values of  $x$ , whereas a polymerized phase is found at higher activities. The transition between those phases is continuous at low values of  $\omega$ , but becomes discontinuous as  $\omega$  is increased. These two regimes are separated by a tricritical point. When the interactions are between bonds (Boltzmann factor  $\kappa$ ), a third phase is stable in part of the parameter space. This phase is a dense phase (all sites are visited by the polymer) and the transition continuous transition line between the non-polymerized and the polymerized phases ends at a critical endpoint. The phase transition between the polymerized and the dense phases may be continuous or not, a tricritical point being found on this transition line. Transfer matrix calculations for this model on the square lattice suggest that this picture may be observed there as well [12].

We solve a model of interacting self-avoiding walks on Husimi lattices (core of the Husimi trees), built with squares [3]. At each site of the lattice the ramification of squares is equal to  $\sigma$ , and therefore the coordination number will be  $q = 2(\sigma + 1)$ . Solutions of models on such lattices may be considered approximations to the solution on hipercubic lattices of the same coordination number, so that a Husimi lattice with  $\sigma = 1$  leads to a solution which approximates the one on a square lattice, the solution for  $\sigma = 2$  may be an approximation for the solution on the cubic lattice, and so on. The Husimi lattice solution may be considered to be the third member of a sequence of approximations whose first two are regular mean-field and Bethe lattice solutions. In a mean-field calculation no correlations are taken into account, while Bethe lattice and Husimi lattice solutions short range correlations are taken care of. It should be stressed, however, that all these solutions lead to classical critical exponents. In some cases, it has been shown that Bethe and Husimi lattice solutions may show features of the phase diagram of models on regular lattices which are not present in the corresponding mean-field approximations [4, 13, 14, 15].

The model we consider is of self-avoiding walks on a Husimi tree, with the initial and final monomer of each walk located at the surface of the tree, so that the density of endpoint monomers in the core of the tree is always

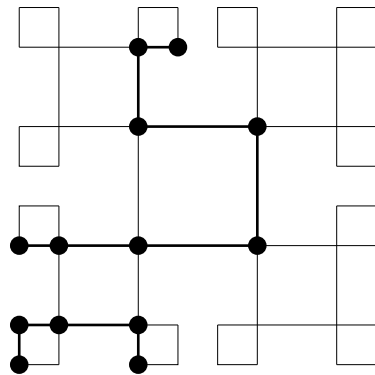


FIG. 1: A Husimi tree with  $\sigma = 1$  and three generations with two polymers on it. The statistical weight of this configuration is equal to  $x^{11}\omega^3\kappa^2$ .

equal to zero. We associate an activity  $x$  to each bond of a walk, and include an interaction energy  $\epsilon_m$  for each pair of monomers on first neighbor sites of the lattice with no bond of the walk between them. Also, an interaction energy  $\epsilon_b$  is associated to each pair of bonds located on opposite edges of elementary squares. The grand partition function of the model on a lattice with  $N$  sites may be written as

$$Y(x, \omega, \kappa; N) = \sum x^{N_b} \omega^{N_{im}} \kappa^{N_{ib}}, \quad (1)$$

where the sum is over all configurations of the walks on the lattice,  $N_b$  is the number of bonds in the configuration,  $N_{im}$  is the number of pairs of interacting monomers, and  $N_{ib}$  is the number of interacting bonds. The Boltzmann factors which correspond to the interactions are given by  $\omega = \exp(-\epsilon_m/k_B T)$  and  $\kappa = \exp(-\epsilon_b/k_B T)$ . A configuration of walks and the corresponding statistical weight may be found in Fig. 1.

## II. SOLUTION OF THE MODEL ON THE HUSIMI TREE

To solve the model on the Husimi lattice we use a recursive procedure, defining subtrees of the Husimi tree and establishing recursion relations between the partial partition functions of the model on the subtrees, for fixed configurations of the root site. Fig. 2 shows the three possible root configurations of a subtree, labeled by the number of bonds incident at the root site from above, and a diagram illustrating how to obtain the partial partition functions of a  $(n + 1)$ -generations subtree from the partial partition functions of  $n$ -generations subtrees. Initially, we consider three subcases for the root configuration with no incident bond, defined by the number of monomers in the first neighbor sites to the root site (0, 1, or 2). To obtain the recursion relations for  $g_{0,0}$ ,  $g_{0,1}$ ,  $g_{0,2}$ ,  $g_1$ , and  $g_2$ , we consider all the possibilities of attaching three sets of  $\sigma$   $n$ -generations subtrees to the vertices

of the elementary square at the root of the new  $(n + 1)$ -generations subtree. The recursion relations are obtained so that the activity of the bonds and the Boltzmann factors of the interactions between monomers and bonds in the elementary square at the root of the new  $(n + 1)$ -generations subtree are considered in the iteration. We then notice that the partial partition functions for the configuration with no incident bond appear in only two combinations in the recursion relations, which are:

$$g_0 = g_{0,0} + g_{0,1} + g_{0,2} \quad (2)$$

and

$$g_3 = g_{0,0} + \omega g_{0,1} + \omega^2 g_{0,2}. \quad (3)$$

If we call  $g_i$ ,  $i = 0, 1, 2, 3$  the partial partition functions of the model defined on an  $n$ -generations subtree and  $g'_i$  the same functions on a  $n + 1$ -generations subtree, we may write the recursion relations as

$$g'_0 = g_0^{3\sigma} + 3Hg_0^{2\sigma} + (1 + 2\omega)H^2g_0^\sigma + 2xF^2g_0^\sigma + \omega^2H^3 + 2x\omega F^2H + x^2F^2g_3^\sigma, \quad (4a)$$

$$g'_1 = 2xF(g_0^{2\sigma} + 2\omega Hg_0^\sigma + \omega^3H^2 + xg_0^\sigma g_3^\sigma + x\omega^2Hg_3^\sigma + x^2\omega\kappa g_3^{2\sigma} + x\omega^2\kappa F^2), \quad (4b)$$

$$g'_2 = x^2F^2(g_0^\sigma + \omega^2H + 2x\omega\kappa g_3^\sigma), \quad (4c)$$

$$g'_3 = g_0^{3\sigma} + 3Hg_0^{2\sigma} + 2\omega(Hg_0^{2\sigma} + \omega H^2g_0^\sigma + xF^2g_0^\sigma) + \omega^2(H^2g_0^\sigma + \omega^2H^3 + 2x\omega F^2H + x^2F^2g_3^\sigma); \quad (4d)$$

where

$$F = \sigma g_1 g_3^{(\sigma-1)}, \quad (5)$$

and

$$H = \sigma g_2 g_3^{(\sigma-1)} + \frac{\sigma(\sigma-1)}{2} g_1^2 g_3^{(\sigma-2)}. \quad (6)$$

It is convenient to define the ratios

$$a = \frac{g_1}{g_0}, \quad b = \frac{g_2}{g_0}, \quad \text{and} \quad c = \frac{g_3}{g_0}, \quad (7)$$

which obey the following recursion relations

$$a' = 2xf(1 + 2\omega h + \omega^3 h^2 + xc^\sigma + x\omega^2 c^\sigma h + x^2\omega\kappa c^{2\sigma} + x\omega^2\kappa f^2)/q, \quad (8a)$$

$$b' = x^2 f^2 (1 + \omega^2 h + 2x\omega\kappa c^\sigma)/q, \quad (8b)$$

$$c' = (1 + h + 2\omega h + 3\omega^2 h^2 + 2\omega x f^2 + \omega^4 h^3 + 2x\omega^3 f^2 h + x^2\omega^2 c^\sigma f^2)/q, \quad (8c)$$

where

$$f = \sigma a c^{(\sigma-1)}, \quad (9a)$$

$$h = \sigma b c^{(\sigma-1)} + \frac{\sigma(\sigma-1)}{2} a^2 c^{(\sigma-2)}, \quad \text{and} \quad (9b)$$

$$q = 1 + 3h + (1 + 2\omega)h^2 + 2xf^2 + \omega^2 h^3 + 2x\omega f^2 h + x^2 c^\sigma f^2. \quad (9c)$$

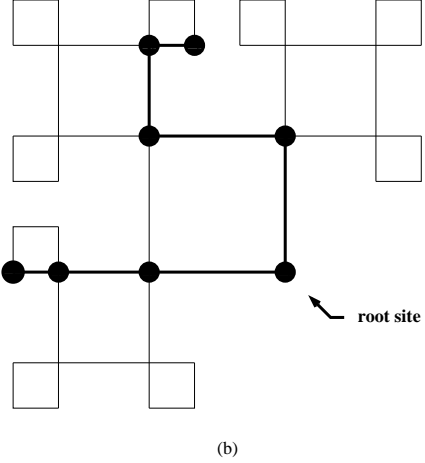
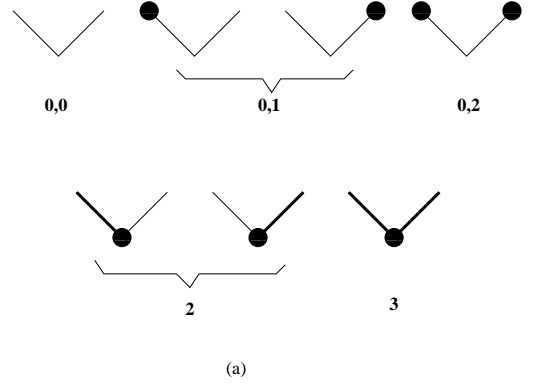


FIG. 2: (a) The possible configurations of the root site of a subtree. (b) A 3-generations subtree is built attaching three 2-generations subtrees to the vertices of the new root square. In this example  $\sigma = 1$ . Two 2-generation subtrees have root configuration 1, while the other one has root configuration 0,0. The resulting root configuration of the 3-generations subtree is 2.

The partition function of the model on the Husimi tree may then be obtained if we consider the operation of attaching four sets of  $\sigma$  subtrees to the central square of the tree. In Fig. 3 the contributing configurations of the central square are shown in the order of the corresponding monomials appearing in the resulting expression below

$$Y_n(x, \omega, \kappa) = g_0^{4\sigma} + 4g_0^{3\sigma}H + 2g_0^{2\sigma}H^2 + 4\omega g_0^{2\sigma}H^2 + 4xg_0^{2\sigma}F^2 + 4\omega^2g_0^\sigma H^3 + 8x\omega g_0^\sigma F^2H + 4x^2g_0^\sigma g_3^\sigma F^2 + \omega^4H^4 + 4x\omega^3F^2H^2 + 2\kappa x^2\omega^2F^4 + 4x^2\omega^2g_3^\sigma F^2H + 4x^3\omega\kappa g_3^{2\sigma}F^2. \quad (10)$$

We expect the thermodynamic behavior of the model on the Husimi tree to be quite different from the one found on regular lattices, since the surface sites dominate in the thermodynamic limit, when the number of iterations  $n \rightarrow \infty$  [16]. We therefore will focus our attention on the behavior in the central region of the tree, which we will refer to as the Husimi lattice[3]. Considering the

contributions to the partition function in Eq. 10, we may calculate the mean numbers of bonds, monomer-monomer interactions and bond-bond interactions in the central square of the tree, which are given by

$$\rho_b = 4xf^2(1 + 2\omega h + 2xc^\sigma + \omega^3 h^2 + \kappa x\omega^2 f^2 + 2x\omega^2 hc^\sigma + 3x^2\omega\kappa c^{2\sigma})/d, \quad (11a)$$

$$\rho_{mm} = 4\omega(h^2 + 2\omega h^3 + 2xf^2 h + \omega^3 h^4 + 3x\omega^2 f^2 h^2 + \kappa x^2 \omega f^4 + 2x^2 \omega f^2 hc^\sigma + x^3 \kappa f^2 c^{2\sigma})/d, \quad (11b)$$

$$\rho_{bb} = 2x^2 \omega \kappa f^2 (\omega^2 f^2 + 2xc^{2\sigma})/d; \quad (11c)$$

where

$$d = 1 + 4h + 2h^2 + 4\omega h^2 + 4xf^2 + 4\omega h^3 + 8x\omega f^2 h + 4x^2 c^{2\sigma} + \omega^4 h^4 + 4x\omega^3 f^2 h^2 + 2\kappa x^2 \omega^2 f^4 + 4x^2 \omega^2 c^\sigma f^2 h + 4x^3 \omega \kappa c^{2\sigma} f^2, \quad (12)$$

calculated at the fixed point of the recursion relations (Eqs. 8).

The thermodynamic behavior of the model is determined by the fixed points of the recursion relations Eqs. 8, each of which correspond to a thermodynamic phase. We investigated the stability regions for each of the fixed points we found, which are three, in general: (a)  $a = b = 0$ ,  $c = 1$ , the non-polymerized fixed point, corresponding to  $\rho_b = \rho_{mm} = \rho_{bb} = 0$ , (b)  $a, b, c \neq 0$  and finite, which is the regular polymerized fixed point, where nonzero densities are found, and (c)  $a \rightarrow \infty$ , and  $b, c \neq 0$  and finite, which we call saturated polymerized phase, since  $\rho_b = \rho_{mm} = 2, \rho_{bb} = 1$  in this phase. This latter is stable in a region of the phase diagram only for the four-coordinated Husimi lattice  $\sigma = 1$ , being absent in the phase diagrams of higher coordinated Husimi lattices. To study the stability region of the saturated phase it is convenient to rewrite the recursion relations 8 in terms of the following new variables:

$$\alpha = \frac{g_0}{g_1}, \quad (13a)$$

$$\beta = \frac{g_2}{g_1}, \quad (13b)$$

$$\text{and } \gamma = \frac{g_3}{g_1}. \quad (13c)$$

In these variables, the saturated fixed point is located at the origin ( $\alpha = \beta = \gamma = 0$ ).

The stability regions of phases (a) and (c) may be found analytically, due to their simplicity. At the stability limit of the non-polymerized phase the largest eigenvalue of the jacobian associated to the recursion relations 8 calculated at the fixed point ( $a, b = 0$  and  $c = 1$ ) is equal to unity. The result is:

$$\kappa \leq \frac{1 - 2x\sigma - 2x^2\sigma}{2x^3\sigma\omega}. \quad (14)$$

while the stability region of the dense polymerized fixed point is obtained in a similar way using the recursion relations written in the other set of variables 13. One obtains ( $\sigma = 1$ ):

$$x \geq \frac{-1 + 8\kappa + \omega - 8\kappa\omega + 4\kappa^2\omega}{\kappa\omega^3(1 - 8\kappa + 4\kappa^2)}. \quad (15)$$

It should be remarked that for  $\kappa = 1 + \sqrt{3/4} \approx 1.86$  the second member of the inequality above diverges, so that the dense phase is never stable for  $\kappa \leq 1 + \sqrt{3/4}$ . In particular, this is true for the model with interactions between monomers only ( $\kappa = 1$ ), as remarked by Pretti [10]. The stability limit of the regular polymerized phase (b) may be found numerically.

The critical surfaces in the phase diagrams will eventually end at tricritical lines. These lines may be obtained requiring the corresponding solution to be a double root of the fixed point equations. Some algebra furnishes the tricritical condition for the (a)-(b) critical surface:

$$P(\omega, x) = -\omega + 7x - 2\omega x - 16x^2 + 10\omega x^2 - 4(\omega - 2)\omega x^3 + 8(1 + (\omega - 1)\omega)x^4 + 2(1 + 2\omega(\omega - 1))x^5 = 0. \quad (16)$$

A similar calculation for the tricritical condition on the critical surface where phases (b) and (c) are equal leads to:

$$\begin{aligned} \mathcal{P}(\omega, \kappa) = & -2(\omega - 1)^2 + (-1 + \omega)^2(63 + 2\omega + \omega^2)\kappa - \\ & 8(99 - 188\omega + 85\omega^2 + 4\omega^4)\kappa^2 + \\ & 16(311 - 553\omega + 217\omega^2 + 25\omega^4)\kappa^3 - \\ & 32(498 - 786\omega + 213\omega^2 + 76\omega^4)\kappa^4 + \\ & 16(1483 - 1876\omega - 44\omega^2 + 454\omega^4)\kappa^5 - \\ & 128(112 - 120\omega - 65\omega^2 + 76\omega^4)\kappa^6 + \\ & 128(9 - 22\omega - 42\omega^2 + 50\omega^4)\kappa^7 - \\ & 1024\omega^2(-1 + 2\omega^2)\kappa^8 + \\ & 256\omega^4\kappa^9 = 0. \end{aligned} \quad (17)$$

To obtain the phase diagrams of the model, in the parameter space defined by  $x$ ,  $\omega$ , and  $\kappa$ , we find which fixed point is stable at each point of the parameter space. Surfaces of this space where the stability limits of two phases are coincident are critical surfaces, and regions where more than one fixed point is stable are related to first order transitions. To obtain the location of these transitions one may use a Maxwell construction, although it is sometimes possible to find the free energy of the model on a treelike lattice using appropriate recursion relations [4]. Due to the simplicity of the non-polymerized and saturated phases, the partition function per elementary square of the lattice may easily be calculated, and this result simplifies considerably the determination of the coexistence surface of these two phases. Since in the non-polymerized phase only configuration 1 of figure 3 is present in the core of the lattice, the partition function per elementary square will be  $y_{np} = 1$ . In the saturated

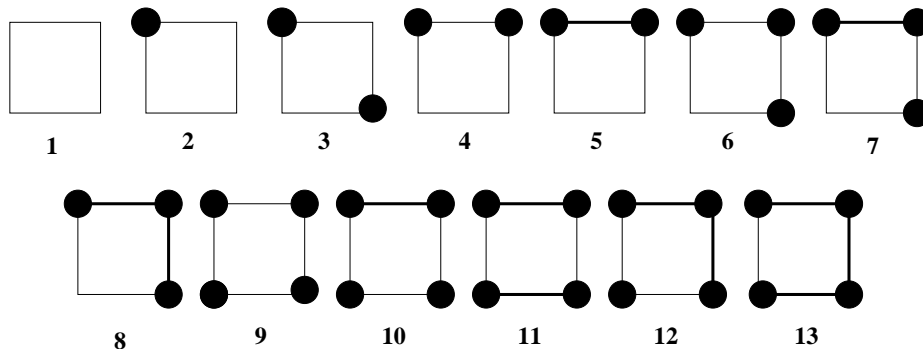


FIG. 3: Possible configurations of the central square of the tree. Each of them contributes with a monomial in the calculation of the partition function of the model on the Husimi tree.

phase, configuration 11 will dominate, and therefore for this phase we have  $z_s = 2\kappa x^2 \omega^2$ . Thus, for the four-coordinated lattice the coexistence surface, in the region where phases (a) and (c) are stable, is given by:

$$2\kappa x^2 \omega^2 = 1. \quad (18)$$

Since the phases (a) and (c) have different densities, the transition between them is always of first order, as may be verified in the phase diagrams below.

### III. PHASE DIAGRAMS

As mentioned before, for  $\sigma \geq 2$  only the non-polymerized and the regular polymerized fixed points of the recursion relations (Eqs. 8) are stable, and therefore no dense polymerized phase appears in the phase diagram. The non polymerized phase is stable for small values of the activity  $x$ , and as the activity is increased, eventually the regular polymerized phase becomes stable. The stability limits of both phases are coincident at low values of the interaction ( $\omega$  and  $\kappa$  close to one), and thus the phase transition between them is continuous. As the strength of the interaction is increased, however, the transition will become discontinuous, and thus the critical surface (where the both phases have the same densities) is separated by a tricritical line from the surface where both phases coexist. This phase diagram, where the collapse transition corresponds to a tricritical point, is expected for this problem since the theta point was recognized as a tricritical point in the pioneering work by de Gennes ([5]), and thus we will concentrate now on the case of the four coordinated lattice.

For  $\sigma = 1$  the dense phase is stable in part of the phase diagram, and therefore richer phase diagrams are obtained. We will consider here constant  $\omega$  cuts of the phase diagram. Perhaps the most interesting constant  $\kappa$  diagram is the one with interactions between monomers only ( $\kappa = 1$ ), which may be found in figure 2 in the comment by Pretti [10]. Essentially three different types of phase diagrams are found in the  $(x, \kappa)$  plane for increasing values of  $\omega$ .

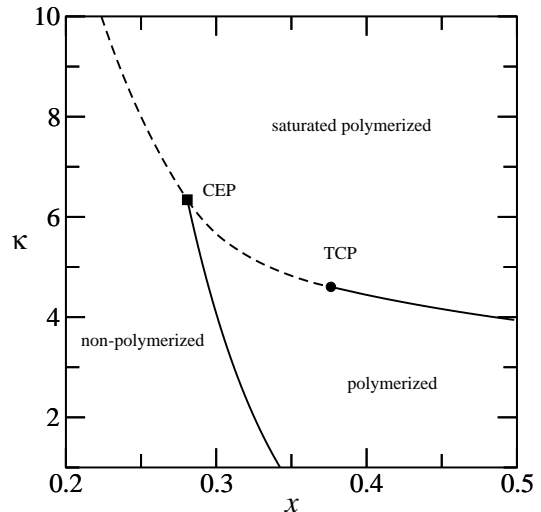


FIG. 4: Phase diagrams of the model for  $\sigma = 1$  and  $\omega = 1$ . Continuous lines are second order transitions and dashed lines are first order transitions. Tricritical points are indicated by circles and critical endpoints are represented by squares.

1. For  $1 \leq \omega \leq \omega_1$  the critical polymerization line ends at a critical endpoint located at the confluence of the coexistence lines of the dense phase with the other two. The particular case with interactions between bonds only ( $\omega = 1$ ) is depicted in figure 4. The dense phase and the regular polymerized phase are separated by a transition line which may be of first or second order, a tricritical point separating these two cases. The critical endpoint becomes a tricritical point at  $\omega_1 \simeq 1.15301$ ,  $\kappa_1 \simeq 4.46985$ ,  $x_1 \simeq 0.29007$ . These values may be obtained noting that this point in the parameter space is located on the coexistence surface of the non-polymerized and the dense phases (equation 18), and on the tricritical line, defined by the stability limit of the non-polymerized phase (equation 14 as an equality) and the tricritical condition (equation 16).

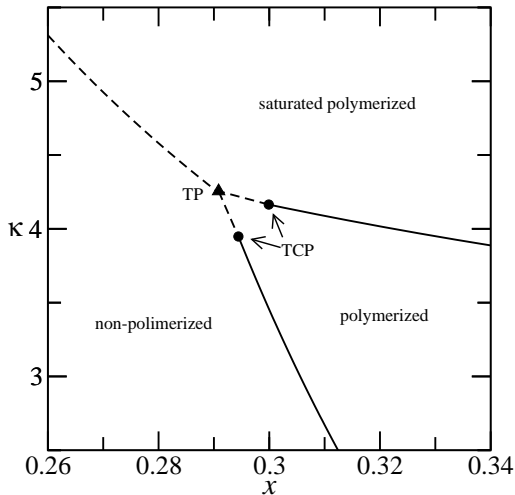


FIG. 5: Phase diagrams of the model for  $\sigma = 1$  and  $\omega = 1.18$ . The triple point is indicated by a triangle.

2. For  $\omega_1 < \omega < \omega_2$  tricritical points are present on the boundaries of the polymerized phase with both the non-polymerized and the dense phases. Three coexistence lines meet at a triple point, as may be seen in figure 5. As  $\omega$  is increased, the tricritical point on the boundary between the polymerized and the dense phases moves closer to the triple point. These two points meet, becoming a critical endpoint, at  $\omega_2 \simeq 1.21717$ ,  $\kappa_2 \simeq 4.08985$ ,  $x_2 \simeq 0.28726$ .
3. For  $\omega \geq \omega_2$  the transition between the polymerized and dense phases is always continuous, and this critical line ends at a critical endpoint. An example is shown in figure 6. The boundary between the non-polymerized and the polymerized phases displays a tricritical point if  $\omega < 1.54508$  and is always of first order for higher values of  $\omega$ .

For the determination of the first order boundaries involving the regular polymerized phase, a Maxwell construction was done using the pair of conjugated variables  $\kappa$  and  $\rho_{bb}$ . Other options are possible, this one was chosen for simplicity. The result of this calculation is not expected to depend on the choice of the variables. For a similar model the Maxwell relations were tested explicitly [17] and also the free energy was obtained directly using a proper iterative procedure [4].

#### IV. CONCLUSION

The solution of models for polymers with attractive interactions on Husimi lattices built with squares leads to the expected phase diagrams when the ramification of the lattice  $\sigma$  is equal or larger to 2. In this case, only one polymerized phase is found, separated from the

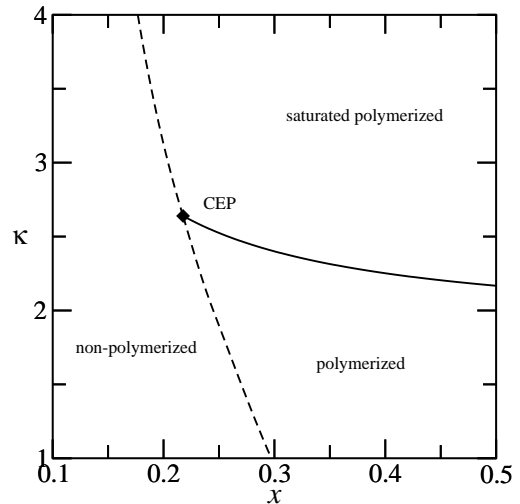


FIG. 6: Phase diagrams of the model for  $\sigma = 1$  and  $\omega = 2$ . Since  $\omega > 1.54508$  the transition between the non-polymerized and the polymerized phase is always of first order.

non-polymerized phase by a first- or second order transition line. The two lines are separated by a tricritical point, which is associated to the collapse transition of the polymers. At a four-coordinated Husimi lattice ( $\sigma = 1$ ), however, a second polymerized phase is stable at high values of the Boltzmann factor  $\kappa$  of the interactions between bonds. Since in this phase all sites of the lattice are incorporated into the polymers, we called it dense polymerized phase.

The phase diagrams obtained for the model on the four coordinated Husimi lattice may offer an explanation for apparently conflicting results in the literature related to the collapse transition of polymers on the square lattice. Transfer matrix and finite size scaling calculations of a model with interactions between *monomers* on first neighbor sites [8] lead to compelling evidences that, as  $\omega$  is increased, the critical polymerization line ends at a tricritical point, but exact Bethe ansatz arguments for a magnetic model which is equivalent to a polymer model with attractive interactions between *bonds* do not indicate a tricritical collapse transition point [7]. In the Husimi lattice solution of the model presented here, the collapse transition point is a tricritical point for the case of interacting *monomers* and a critical endpoint when the interaction is between *bonds*. This is consistent with the results known for these models on the square lattice. It is possible to obtain many features of the problem of *directed* polymers with interacting bonds on the square lattice exactly [18]. Although the collapse transition for this case is also a multicritical point, the details of the phase diagram are quite different from the ones found here. A rather unphysical feature of this model is that a polymerized phase of zero density of monomers occupies a finite region of the phase diagram, even in the absence of any attractive interactions.

It is of some interest to find out how the qualitatively different phase diagrams for interactions between monomers and bonds change into each other. Thus, we considered here a more general model where both interactions are present. We then found that the transition between phase diagrams where the collapse transition is a tricritical point (interactions between monomers) and those where it is a critical endpoint (interaction between bonds) occurs through an intermediate phase diagram where two tricritical points are present and three coexistence lines meet at a triple point. It should be stressed that the two tricritical points found in the phase diagram are not part of the same tricritical line in the full parameter space  $(x, \omega, \kappa)$ . This poses the question if those two distinct tricritical points actually exist for the model defined on two-dimensional lattices and, if this is true, if they share the same set of tricritical exponents. Although experimental studies of the collapse transition of

polymers confined in a two-dimensional surface have been done [19] and seem to confirm the tricritical nature of the transition, monodisperse polymer solutions were used for them, while in our calculations the chains are polydisperse.

### Acknowledgments

We acknowledge Prof. Paulo Murilo C. de Oliveira, for suggesting the study of the model in the extended parameter space. We are grateful to the argentinian agencies CONICET and SECYTUNC, as well as the brazilian agencies CAPES, CNPq, and FAPERJ for partial financial support. PS acknowledges the hospitality of Universidade Federal Fluminense, where part of this work was done.

- 
- [1] P. G. de Gennes, *Scaling Concepts in Polymer Physics*, (Cornell, Ithaca, 1979).
  - [2] R. Baxter, *Exactly Solved Models in Statistical Mechanics*, (Academic Press, London, 1982).
  - [3] K. Husimi, *J. Chem. Phys.* **18**, 682 (1950); J. F. Stilck and M. J. de Oliveira, *Phys. Rev. A* **42**, 5955 (1990).
  - [4] P. Gujrati, *Phys. Rev. Lett.* **74**, 809 (1995).
  - [5] P. G. de Gennes, *J. Physique* **36**, L55 (1975).
  - [6] H. W. J. Blöte and B. Nienhuis, *J. Phys. A* **22**, 1415 (1989).
  - [7] M. T. Batchelor, B. Nienhuis, and S. O. Warnaar, *Phys. Rev. Lett.* **62**, 2425 (1989); B. Nienhuis, *Physica A* **163**, 152 (1990).
  - [8] B. Derrida and H. Saleur, *J. Phys. A* **18**, L1075 (1985); H. Saleur, *J. Stat. Phys.* **45**, 419 (1986).
  - [9] J. F. Stilck, K. D. Machado, and P. Serra, *Phys. Rev. Lett.* **73**, 2734 (1996).
  - [10] M. Pretti, *Phys. Rev. Lett.* **89**, 169601 (2002).
  - [11] J. F. Stilck, P. Serra, and K. D. Machado, *Phys. Rev. Lett.* **89**, 169602 (2002).
  - [12] K. D. Machado, M. J. de Oliveira, and J. F. Stilck, *Phys. Rev. E* **64**, 051810 (2001).
  - [13] J. F. Stilck and J. C. Wheeler, *Physica A* **190**, 24 (1992).
  - [14] A. J. Banchio y P. Serra, *Phys. Rev. E* **51**, 2213 (1995).
  - [15] M. Pretti, *Phys. Rev. E* **66**, 061802 (2002).
  - [16] E. Müller-Hartmann and J. Zittartz, *Phys. Rev. Lett.* **33**, 893 (1974).
  - [17] J. F. Stilck and J. C. Wheeler, *J. Stat. Phys.* **46**, 1 (1987).
  - [18] P.-M. Binder, A. L. Owczarek, A. R. Veal, and J. M. Yeomans, *J. Phys. A* **23**, L975 (1990).
  - [19] R. Vilanove and F. Rondelez, *Phys. Rev. Lett.* **45**, 1502 (1980).